Thermophysics and Aeromechanics, *2021*, *Vol. 28*, *No. 5*

DOI: 10.1134/S0869864321050176

On the efficiency of using different excitation lines of (1–0) two-line OH fluorescence for planar thermometry*

A.S. Lobasov, R.V. Tolstoguzov, D.K. Sharaborin, L.M. Chikishev, and V.M. Dulin [c]

Kutateladze Institute of Thermophysics SB RAS, *Novosibirsk*, *Russia*

Novosibirsk State University, *Novosibirsk*, *Russia*

E-mail: vmd@itp.nsc.ru [c]

(*Received May 21*, *2021*; *revised July 27*, *2021*;
accepted for publication July 30, *2021*)

The paper presents the results of simulation and experimental study on the efficiency of selecting a pair of excitation lines of OH hydroxyl radical for the (1–0) transition for the $A^2\Sigma^+$–$X^2\Pi$ system for local temperature measurement in a hydrocarbon flame. The LASKIN software was used for the numerical simulation. The temperature field for a laminar methane-air premixed flame (with equivalence ratio equal 1.1) at the atmopsheric pressure was measured. Different combinations of literature-recommended pairs of excitation lines were considered. The results of numerical simulation agree with a theoretical dependency for the temperature range of 1200 – 2100 K for the coupled excitation lines $Q_1(5)$:$Q_1(14)$ and $Q_1(5)$:$Q_2(11)$. However, a moderate discrepancy is observed for the pairs $R_2(2)$:$R_2(13)$ and $R_2(2)$:$R_2(10)$. It is concluded that the coupled excitation of $Q_1(5)$:$Q_1(14)$ and $R_2(2)$:$R_2(13)$ lines provide a higher sensitivity to the temperature variation. The benefit of the latter pair is that these transitions correspond to close values of the excitation wavelengths in the vicinity of 282 nm. Therefore, this can be convenient for the arrangement of experiments.

Keywords: planar thermometry, laser-induced fluorescence, hydroxyl radical.

The method of Planar Laser-Induced Fluorescence (PLIF) is widely used for the diagnostics of flows. This method is based on the imaging of the local molecular fluorescence intensity which is induced by a laser in a selected plane of the flow. For flows with combustion, the varying of laser wavelength makes possible the exciting different types of reactive molecules (hydrocarbons and O_2), intermediates (HCHO, HCO, CH, CO, OH, etc.) or combustion products (NO, NO_2). The technique is used also for the tracking of reaction-inert molecules (I_2, SO_2). In particular, the PLIF technique is often used for the analysis of the spatial distributions of radicals and for the visualization of the hot zones or local regions with chemical reactions [1–3]. The PLIF method can be used also for non-intrusive measurements of temperature fields in reacting or non-reacting gaseous flows. For example, NO is used for the temperature measurements in high-speed flows [4] and in flows with combustion at high temperatures (up to 2300 K) [5].

* Research was supported by the Ministry of Education and Science of Russia, Agreement No. 075-15-2020-806.

For the case of a steady laminar flame, the scanning of the excitation wavelength for NO fluorescence (with concentration up to 2000 ppm) offers the 2D temperature field measurements (up to ~ 2200 K) with the accuracy better than 10 % [6]. The limitation of this approach is a long time of the measuring procedure; therefore, it can be applied to steady flows only. A similar PLIF-based thermometry approach relies on the fluorescence excitation for two different transitions. This approach, unlike the wavelength scanning, provides a lower accuracy, but a better time resolution and can be applied to study turbulent flames (only two laser pulses are needed). The 2D [7, 8] and 3D [9] visualization of almost instant temperature distributions is possible through OH fluorescence registration (excitation for two separate bands [10]). These two approaches (excitation of two bands or scanning of OH fluorescence spectrum) for measuring temperature fields had been discussed in [11].

In general, this two-line OH PLIF method is based on the recording the ratio of fluorescence intensities while exciting two transitions into one upper state. Typically, the PLIF with excitation of OH (hydroxyl radical) (1–0) band for the wavelengths near 282 nm and recording the intensity of (1–1) and (0–0) bands within the range 300 – 320 nm is used. Since the selection rules put limits on the rotational quantum number, the temperature sensitivity of the method is low, when the excitation is performed for two close initial states in the oscillation band (1–0). Therefore, the method is used for the excitation transitions not overlapping with the other ones. In particular, $R_2(10)$, $R_1(12)$, $R_2(2)$, $R_2(13)$, $Q_1(5)$ lines are used near 282 nm and $Q_2(11)$ and $Q_1(14)$ lines near 286 nm. Sometimes, the spectral lines overlapping with other lines are used, e.g., $P_1(2)$ which is near $R_1(14)$, or $R_2(8)$ which is near $R_2(5)$. The common practice is to use the ratio of the fluorescent intensities of the pair lines $P_1(2)$:$R_2(13)$ and $Q_1(5)$:$Q_1(14)$ (see [7, 10] and [9, 11]) and also the pairs $P_1(2)$:$Q_2(11)$, $Q_1(5)$:$Q_2(11)$, $P_1(1)$:$R_1(14)$, $R_2(8)$:$Q_2(11)$ [11–13]. Different publications offer controversial conclusions about the efficiency of the different paired bands for the temperature measurements.

In this paper, we performed a numerical and experimental study for the efficiency of using the most popular combinations of the excitation lines ($Q_1(5)$:$Q_1(14)$, $P_1(2)$:$R_2(13)$) and less common combinations ($R_2(2)$:$R_2(13)$, $R_2(2)$:$R_2(10)$) for the band $A^2\Sigma^+$–$X^2\Pi$ (1–0) while recording the fluorescence intensity for spectral transitions (0–0) and (1–1). The LASKIN software was used for the numerical simulation of OH fluorescence [14]. The experiments were performed for a laminar premixed methane-air flame (with an equivalence ratio $\Phi = 0.9$). The fuel-air mixture is supplied from a profiled axisymmetric nozzle with the outlet diameter of $d = 15$ mm. The axial mean flow velocity at the nozzle exit was $U_0 = 1$ m/s, and the Reynolds number was Re = 1000. The PLIF recording system consisted of a tunable pulse dye laser (Sirah Precision Scan), a pulsed pump Nd:YAG laser (Quanta-Ray), and a Princeton Instruments PI-MAX-4 intensified CCD camera (1 Mpixel, 16 bit, S20 photocathode), with a fused silica lens and a band-pass optic filter (310 ± 10 nm).

Another set of optic lenses converted the laser beam into a collimated laser sheet with the width of 50 mm and thickness of 0.8 mm. The average laser pulse energy (emission at 281 – 285 nm wavelength) was about 20 mJ. The linear mode of fluorescence was checked by varying the laser emission power. The problem of accounting for the nonuniform laser energy distribution and pulsations of the laser energy was solved by redirecting a part of the laser beam power (5 %) by reflecting it by using a quarts plate into a calibration cuvette (filled with a 6G rhodamine solution). The spatial distribution of the fluorescent signal inside the cuvette was recorded using a CCD camera (ImperX Bobcat IGV-B4820, 16 Mpixel, 12 bit).

Figure 1 presents the ratio of fluorescence signals integrated for the range 300 – 320 nm taken for different excitation pairs. The symbols are the simulation data using the LASKIN software, and the curves are the analytical functions for the signals ratio vs. temperature which are based on equation:

$$R = \frac{S_1}{S_2} = \frac{B_1 I_1 (2J_1 + 1)}{B_2 I_2 (2J_2 + 1)} \exp\left(-\frac{E_1 - E_2}{kT} \right), \quad (1)$$

where R is the ratio of fluorescence signals (S_2 and S_1) excited by different transitions, I is the energy of the laser pulse, B is the Einstein absorption coefficient for the ground state, J is the rotational angular momentum quantum number, E_1 and E_2 are the energy levels of the excited states, k is the Boltzmann constant, and T is the temperature. The energies of ground states E_1 and E_2 are taken from [15]. The vertical dashes on the analytical lines depict the limits of the range of the experimental data available for this particular pair of transitions.

The graphs indicate that the best matching between the results of the numerical simulation and theoretical formula takes place for these pairs: $Q_1(5)$:$Q_1(14)$ and $Q_1(5)$:$Q_2(11)$. For them, the discrepancy is below 7 % for the temperature range 1200 – 2100 K. Meanwhile, the $Q_1(5)$:$Q_1(14)$ pair demonstrates the higher sensitivity for this interval (the intensity ratio varies by four times for the interval 1200 – 2100 K). The data for $R_2(2)$:$R_2(13)$ and $R_2(2)$:$R_2(10)$ pairs also demonstrate a good compliance with the experimental data in this temperature interval: the discrepancy is less than 14 % while providing a high temperature sensitivity for $R_2(2)$:$R_2(13)$ pair. Although the $P_1(2)$:$R_2(13)$ and $P_1(2)$:$Q_2(11)$ pairs demonstrate a high sensitivity, the discrepancy between the simulation and theory is much higher.

The PLIF error can be decomposed into a precision (the random error related to signal-to-noise ratio) and accuracy (a systematic error, including the calibration inaccuracy). In this study, we use a single-detector registration scheme, correct for the radiation energy within the laser sheet and subtract the background. Therefore, the systematic error from the detector is considered much lower than that of the calibration. For the improvement of the signal-to-noise ratio, the images can be averaged. As a result, the actual signal-to-noise ratio was higher than 30:1. Thus, the random part of error was below 5 % of the measured value. The publications [16, 17] offer a detailed analysis of error sources occurring in the temperature-and-concentration measurements for the flame (the technique of Spontaneous Raman Scattering – SRS). These data give the standard deviation of the measured temperature by the method [18] as a value of about 10 %.

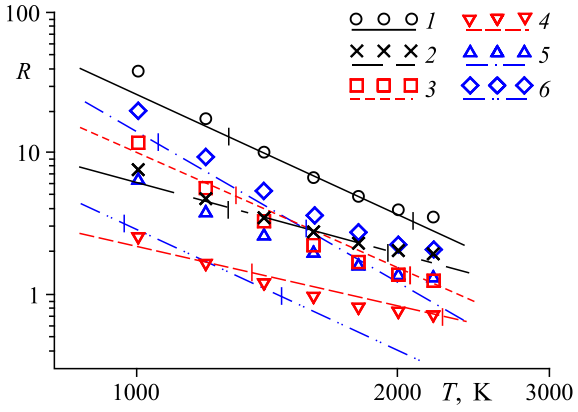

Fig. 1. The OH fluorescence ratios for different excitation transition pairs of the (1–0) band in $A^2\Sigma^+$–$X^2\Pi$ system.
1 — $Q_1(5)$:$Q_1(14)$, *2* — $Q_1(5)$:$Q_2(11)$, *3* — $R_2(2)$: $R_2(13)$, *4* — $R_2(2)$:$R_2(10)$, *5* — $P_1(2)$:$Q_2(11)$, *6* — $P_1(2)$:$R_2(13)$.

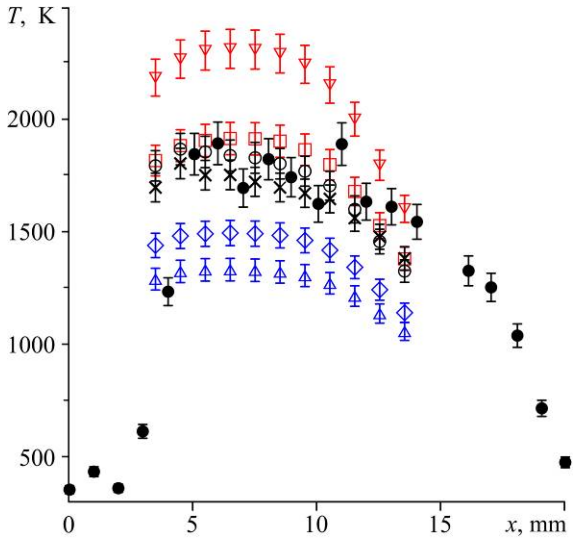

Fig. 2. Comparison between the local temperature values estimated from two-line OH PLIF and SRS [18] (filled symbols). Symbols are taken from Fig. 1.

Figure 2 shows the temperature profiles (at 22.5 mm from the nozzle exit) calculated from experimental PLIF data and similar data measured by the SRS technique [18]. The data for the $R_2(2)$:$R_2(10)$ pair provide a significant overestimation of the temperature (even compared to the adiabatic temperature 2118 K for this fuel-air mixture): this might be explained by a low sensitivity for this pair. For the spectral pairs $P_1(2)$:$R_2(13)$ and $P_1(2)$:$Q_2(11)$, the temperature is underestimated. Probably, this is due to the fact that $P_1(2)$ line is close to $R_1(14)$ line and the excitation of two transitions generates a high calibration error. For the set of lines ($Q_1(5)$:$Q_1(14)$, $Q_1(5)$:$Q_2(11)$, and $R_2(2)$:$R_2(13)$), there is a high compliance between the temperature estimates (mismatch is less than 90 K). The minimum values of the detected temperature for all cases are approximately 1350 K.

References

1. **A. Fayoux, K. Zähringer, O. Gicquel, and J. Rolon,** Experimental and numerical determination of heat release in counterflow premixed laminar flames, Proceedings of the Combustion Institute, 2005, Vol. 30, No. 1, P. 251–257.
2. **B.O. Ayoola, R. Balachandran, J.H. Frank, E. Mastorakos, and C.F. Kaminski,** Spatially resolved heat release rate measurements in turbulent premixed flames, Combustion and Flame, 2006, Vol. 144, Nos. 1–2, P. 1–16.
3. **R.L. Gordon, A.R. Masri, and E. Mastorakos,** Heat release rate as represented by [OH]×[CH2O] and its role in autoignition, Combustion Theory and Modelling, 2009, Vol. 13, No. 4, P. 645 – 670.
4. **E.R. Lachney and N.T. Clemens,** PLIF imaging of mean temperature and pressure in a supersonic bluff wake, Experiments in Fluids, 1998, Vol. 24, No. 4, P. 354 –363.
5. **T. Lee, W.G. Bessler, H. Kronemayer, C. Schultz, and J.B. Jeffries,** Quantitative temperature measurements in high-pressure flames with multiline NO-LIF thermometry, Applied Optics, 2005, Vol. 44, No. 31, P. 6718 – 6728.
6. **W.G. Bessler and C. Schulz,** Quantitative temperature measurements in high-pressure flames with multiline NO-LIF thermometry, Applied Optics, 2005, Vol. 44, No. 31, P. 6718 – 6728.
7. **R. Giezendanner-Thoben, U. Meier, W. Meier, and M. Aigner,** Phase-locked temperature measurements by two-line OH PLIF thermometry of a self-excited combustion instability in a gas turbine model combustor, Flow, Turbulence and Combustion, 2005, Vol. 75, No. 1– 4, P. 317–333.
8. **B. Ayoola, G. Hartung, C.A. Armitage, J. Hult, R.S. Cant, and C.F. Kaminski,** Temperature response of turbulent premixed flames to inlet velocity oscillations, Experiments in Fluids, 2009, Vol. 46, No. 1, P. 27– 41.
9. **B.R. Halls, P.S. Hsu, S. Roy, T.R. Meyer, and J.R. Gord,** Two-color volumetric laser-induced fluorescence for 3D OH and temperature fields in turbulent reacting flows, Optics Letters, 2018, Vol. 43, No. 12, P. 2961–2964.
10. **R. Devillers, G. Bruneaux, and C. Schulz,** Development of a two-line OH-laser-induced fluorescence thermometry diagnostics strategy for gas-phase temperature measurements in engines, Applied Optics, 2008, Vol. 47, No. 31, P. 5871–5885.

11. **S. Kostka, S. Roy, P.J. Lakusta, T.R. Meyer, M.W. Renfro, J.R. Gord, and R. Branam,** Comparison of line-peak and line-scanning excitation in two-color laser-induced-fluorescence thermometry of OH, Applied Optics, 2009, Vol. 48, No. 32, P. 6332–6343.
12. **J.M. Seitzman, R.K. Hanson, P.A. DeBarber, and C.F. Hess,** Application of quantitative two-line OH planar laser-induced fluorescence for temporally resolved planar thermometry in reacting flows, Applied Optics, 1994, Vol. 33, No. 18, P. 4000–4012.
13. **E.J. Welle, W.L. Roberts, C.D. Carter, and J.M. Donbar,** The response of a propane-air counter-flow diffusion flame subjected to a transient flow field, Combustion and Flame, 2003, Vol. 135, No. 3, P. 285–297.
14. **A. Bülter, U. Lenhard, U. Rahmann, K. Kohse-Höinghaus, and A. Brockhinke,** Laskin: Efficient simulation of spectra affected by energy transfer, Proceedings of Laser Applications to Chemical and Environmental Analysis (9 February 2004), Optical Society of America, USA, 2014. Paper TuE4.
15. **G.H. Dieke and H.M. Crosswhite,** The ultraviolet bands of OH fundamental data, J. Quantitative Spectroscopy and Radiative Transfer, 1962, Vol. 2, No. 2, P. 97–199.
16. **F. Rabenstein and A. Leipertz,** Two-dimensional temperature determination in the exhaust region of a laminar flat-flame burner with linear Raman scattering, Applied Optics, 1997, Vol. 36, No. 27, P. 6989–6996.
17. **F. Rabenstein and A. Leipertz,** One-dimensional, time-resolved Raman measurements in a sooting flame made with 355-nm excitation, Applied Optics, 1998, Vol. 37, No. 21, P. 4937–4943.
18. **D.K. Sharaborin, D.M. Markovich, and V.M. Dulin,** Planar spontaneous Raman-scattering spectroscopy for reacting jet-flow diagnostics using Lyot–Ehman tunable filter, Techn. Phys. Letters, 2018, Vol. 44, No. 1, P. 53–56.